

Analysis of Flow Past a Porous Rotating Disk with Thermo-Diffusion and Diffusion-Thermo with Convective Boundary Condition

Yusuf, A., Bima, A., Salihu, N. O., Aiyesimi, Y. M. and Jiya, M.

Department of Mathematics, Federal University of Technology, Minna, Niger State, Nigeria

ABSTRACT

Analysis of flow past a porous rotating disk with thermo-diffusion and diffusion-thermo with convective boundary condition are studied and presented in rectangular form Mathematically. These equations are continuity, momentum, temperature and concentration which were reduced to nonlinear coupled ordinary differential equations from their PDE forms. The solution to these reduced equations were solved by introducing Adomian polynomials. The results were validated with the existing literatures and a good agreement was established. The parameters that occur in the solutions were varied on the fluid radial, tangential, axial velocities, temperature and concentration. Thermo-diffusion was found to enhance the fluid temperature while diffusion-thermo also boost the fluid concentration.

Keywords: Boundary layer, Dufour and Soret effect, Ferro hydro dynamics (FHD), Adomian decomposition, rotating disk.

INTRODUCTION

The significance of the study of increase in the fluid chemical reaction (diffusion-thermo) that leads to increase in temperature and increase in temperature that leads to increase in concentration (thermo-diffusion) in a disk rotating fluid can never be over emphasize due to its enormous application in engineering both theoretically and practically. Rotation of the fluid in the disk causes the viscous forces to be balance by Coriolis forces against the forces of inertia. Observing the rotational reference frame, the forces are known as apparent deflection of an object in motion.

Turkylmazoglu (2014) described the effect of Joule heating and viscous dissipation on time-dependent MHD flow over a rotating disk which is radially stretch. Devi and Ganga (2009) studied the heat transfer and viscous dissipation effects on nonlinear MHD flow over a stretching porous surface. The influence of viscous dissipation on radiative heat transfer in MHD flow past a stretching surface has been analyzed by Chen (2010). Maleque (2010) investigated the time dependent flow of an electrically conducting fluid over a rotating disk by taking variable viscosity. By taking viscous dissipation effect and heat source, Sharma (2012) examined an unsteady flow of viscous fluid through a horizontal porous stretching sheet. Recently, Khan and Alzahrani (2021) described the impact of Brownian motion and viscous

dissipation on nonlinear slip flow of Jeffrey nanomaterial over a curved surface. Heat transfer in rotating disk system is of major significance in engineering, for example, gas turbine cooling and computer disk drive Harrero *et al.* (1994). Al-Hadharani (2003) proposed a model for viscous dissipation in a porous medium which is probably adequate for most of the practical purposes. Several Researchers such as Suleiman and Yusuf (2020), Yusuf *et al.* (2021a), Bolarin *et al.* (2019), Yusuf *et al.* (2021b), Aiyesimi *et al.* (2013) have all demonstrated in their work the reliability of the Decomposition method in solving boundary layer problems.

From the literatures available to the researchers, the study of boundary layer flow past a porous rotating disk with thermo-diffusion and diffusion-thermo with convective boundary condition is a new advancement in the literature where ADM was employed to carry out the analysis.

MATERIALS AND METHODS

The flow of a steady laminar flow in a rotating disk with concentration $c = c_w$ and $c \rightarrow c_\infty$ at $z = 0$ and $z \rightarrow \infty$ respectively is considered. Following the formulation in Sharma *et al.* (2021) by incorporating the Dufour and Soret effects with convective boundary conditions. The model formulation is given as:

*Corresponding author. E-mail: yusuf.abdulhakeem@futminna.edu.ng

Author(s) agree that this article remain permanently open access under the terms of the Creative Commons Attribution License 4.0 International license

$$\frac{\partial u}{\partial r} + \frac{u}{r} + \frac{\partial w}{\partial z} = 0 \quad (1)$$

$$-\frac{1}{\rho} \frac{\partial p}{\partial r} + \frac{\mu_0}{\rho} |M| \frac{\partial}{\partial r} |H| + v \left[\frac{\partial^2 u}{\partial r^2} + \frac{\partial}{\partial r} \left(\frac{u}{r} \right) + \frac{\partial^2 u}{\partial z^2} \right] + 2\Omega v - \frac{\mu_\infty}{\rho K} u = u \frac{\partial u}{\partial r} + w \frac{\partial u}{\partial z} - \frac{v^2}{r} \quad (2)$$

$$v \left[\frac{\partial^2 v}{\partial r^2} + \frac{\partial}{\partial r} \left(\frac{v}{r} \right) + \frac{\partial^2 v}{\partial z^2} \right] - 2\Omega u - \frac{\mu_\infty}{\rho K} v = u \frac{\partial v}{\partial r} + w \frac{\partial v}{\partial z} + \frac{uv}{r} \quad (3)$$

$$-\frac{1}{\rho} \frac{\partial p}{\partial z} + \frac{\mu_0}{\rho} |M| \frac{\partial}{\partial z} |H| + v \left[\frac{\partial^2 w}{\partial r^2} + \frac{1}{r} \frac{\partial w}{\partial r} + \frac{\partial^2 w}{\partial z^2} \right] - \frac{\mu_\infty}{\rho K} w = u \frac{\partial w}{\partial r} + w \frac{\partial w}{\partial z} \quad (4)$$

$$\rho c_p \left(u \frac{\partial T}{\partial r} + w \frac{\partial T}{\partial z} \right) = k \left(\frac{\partial^2 T}{\partial r^2} + \frac{1}{r} \frac{\partial T}{\partial r} + \frac{\partial^2 T}{\partial z^2} \right) + \mu \left[\left(\frac{\partial u}{\partial z} \right)^2 + \left(\frac{\partial v}{\partial z} \right)^2 \right] + \frac{D_m K_T}{c_p} \frac{\partial^2 c}{\partial z^2} \quad (5)$$

$$u \frac{\partial c}{\partial r} + w \frac{\partial c}{\partial z} = D_B \frac{\partial^2 c}{\partial z^2} + \frac{D_m K_T}{T_m} \frac{\partial^2 T}{\partial z^2} \quad (6)$$

$$(u, v, w) = \left(0, r\Omega, \frac{v}{\delta} \right), \quad p = p_0, \quad -k \frac{\partial T}{\partial y} = h(T_s - T_\infty), \quad c = c_w \quad \text{as } z=0 \quad (7)$$

$$(u, v, w) \rightarrow (0, 0, 0), \quad p \rightarrow p_\infty, \quad T \rightarrow T_\infty, \quad c \rightarrow c_\infty \quad \text{as } z \rightarrow \infty$$

Where u, v, w are component of velocity fluid, ρ is the density, p is the fluid pressure, M stands for magnetization, H stands for magnetic-field vector, μ is dynamic viscosity, K is Darcy permeability, c_p specific heat capacity, T is the fluid temperature, k is

the thermal conductivity, Ω angular velocity, T_M mean fluid temperature, K_T thermal diffusion ratio, D_M is mean diffusion.

The similarity transformation is given as:

$$\left. \begin{aligned} u &= r\Omega \frac{\partial U}{\partial \eta}, \quad v = r\Omega V, \quad w = \frac{v}{\delta} W, \quad p = \frac{\rho v^2}{\delta^2} P \\ T - T_\infty &= (T_w - T_\infty) \theta, \quad c - c_\infty = (c_w - c_\infty) \phi, \quad \eta = \frac{z}{\delta} \end{aligned} \right\} \quad (8)$$

$$\text{According to [14]} \quad \frac{1}{\rho} \frac{\partial p}{\partial r} = r\Omega^2, \quad |H| = \frac{m}{2\pi r^2}, \quad |M| = k_1 (T_c - T)$$

Where η, U, V, W, P, θ and ϕ corresponds to fluid dimensionless distance, dimensionless radial velocity, dimensionless tangential velocity, dimensionless axial velocity, fluid Pressure, dimensionless temperature and dimensionless fluid concentration respectively. δ stands for scalar factor,

k_1 is pyro magnetic coefficient, T_c stands for curie temperature.

Introducing the similarity transformation in (8) and the linearized equation above into equation (1) to (7), the equations simplify to nonlinear coupled ordinary differential below:

$$\left.
\begin{aligned}
& \frac{\partial^3 U}{\partial \eta^3} - R \left\{ \left(\frac{\partial U}{\partial \eta} \right)^2 - V^2 - 2V + 1 - 2U \frac{\partial^2 U}{\partial \eta^2} + \beta \frac{\partial U}{\partial \eta} + \frac{2B}{\text{Re}^2} \right\} = 0 \\
& \frac{\partial^2 V}{\partial \eta^2} - 2R \left\{ \left(\frac{\partial U}{\partial \eta} V - U \frac{\partial V}{\partial \eta} \right) - \frac{\partial U}{\partial \eta} + \frac{\beta}{2} V \right\} = 0 \\
& \frac{\partial^2 W}{\partial \eta^2} - W \frac{\partial W}{\partial \eta} - R\beta W - \frac{\partial P}{\partial \eta} = 0 \\
& \frac{\partial^2 \theta}{\partial \eta^2} + 2\text{Pr}RU \frac{\partial \theta}{\partial \eta} + \text{Pr}Ec \left[\left(\frac{\partial^2 U}{\partial \eta^2} \right)^2 + \left(\frac{\partial V}{\partial \eta} \right)^2 \right] + Du \frac{\partial^2 \varphi}{\partial \eta^2} = 0 \\
& \frac{\partial^2 \varphi}{\partial \eta^2} + 2RLeU \frac{\partial \varphi}{\partial \eta} + LeSr \frac{\partial^2 \theta}{\partial \eta^2} = 0 \\
& \left. \frac{\partial U}{\partial \eta} \right|_{\eta=0} = 0, \quad V(0) = 1, \quad W(0) = 1, \quad \theta' = -\text{Bt}(1 - \theta), \quad \varphi(0) = 1, \quad \eta = 0 \\
& \left. \frac{\partial U}{\partial \eta} \right|_{\eta=\infty} = V(\infty) = W(\infty) = \theta(\infty) = \varphi(\infty) = 0, \quad \eta \rightarrow \infty
\end{aligned}
\right\} \quad (9)$$

Where $R = \frac{\Omega \delta^2}{\nu}$, $\beta = \frac{\nu \Omega}{K}$, $\text{Re} = \frac{\Omega r^2}{\nu}$, $B = \frac{m \mu_{\infty} k_1 (T_c - T) \rho}{2 \pi \mu_{\infty}^2}$, $\text{Pr} = \frac{\nu \rho c_p}{k}$, $Ec = \frac{r^2 \Omega^2}{(T_w - T_{\infty}) c_p}$,
 $Du = \frac{D_m K_T (c_w - c_{\infty})}{\nu c_p (T_w - T_{\infty})}$, $Le = \frac{\nu}{D_B}$, $Sr = \frac{D_m K_T (T_w - T_{\infty})}{T_m (c_w - c_{\infty}) \nu}$, $\text{Bt} = \frac{h}{\delta k}$.

Are rotational parameter, Darcy number, Reynolds number, FHD interactive parameter, Prandtl number, Eckert number, Dufour number, Lewis number, Soret number and Biot number respectively.

RESULTS AND DISCUSSION

The nonlinear coupled ordinary differential equations with corresponding boundary conditions in equation (9) are highly nonlinear. ADM is employed to obtain the solution. The results obtained are compared with the existing literature and a good agreement are observed as seen in Table 1.

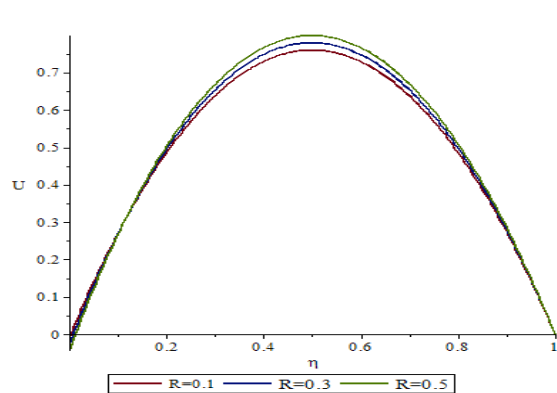


Figure 1: Variation of R on U

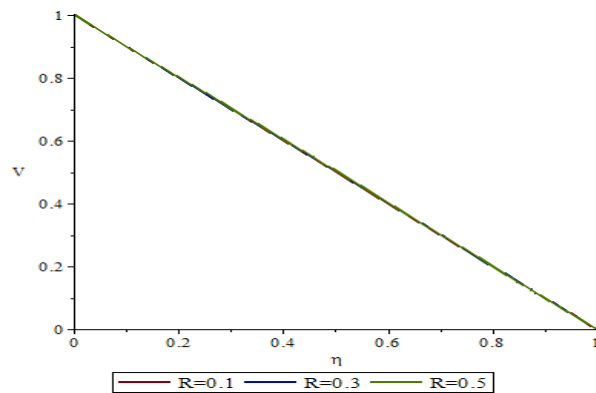


Figure 2: Variation of R on V

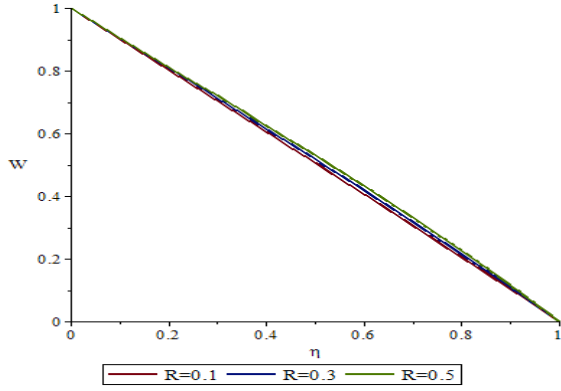


Figure 3: Variation of R on W

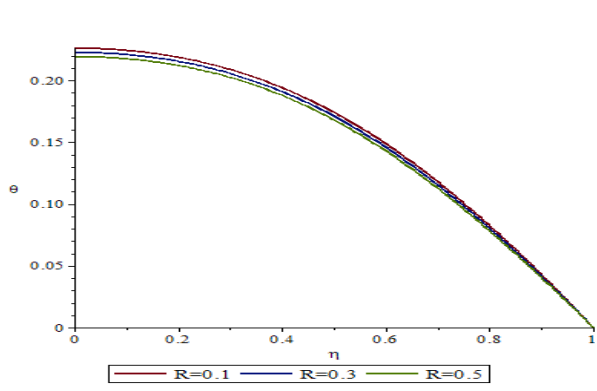


Figure 4: Variation of R on θ

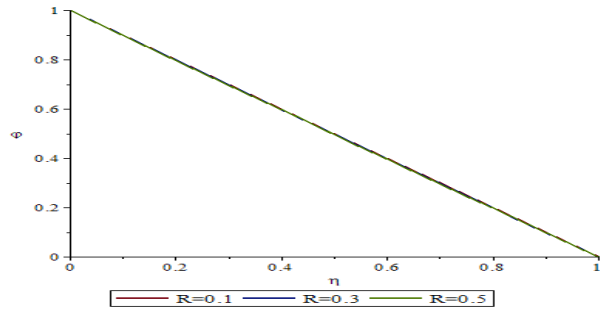


Figure 5: Variation of R on φ

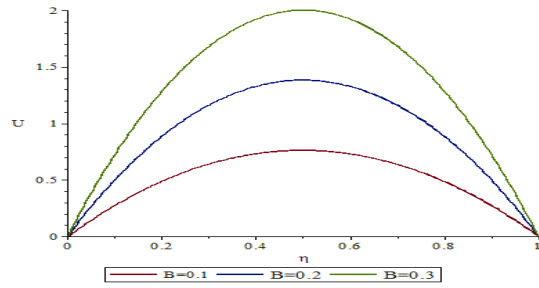


Figure 6: Variation of B on U

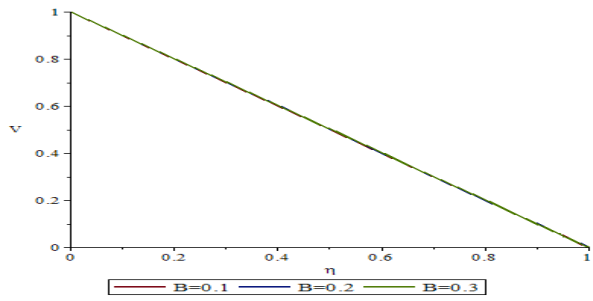


Figure 7: Variation of B on V

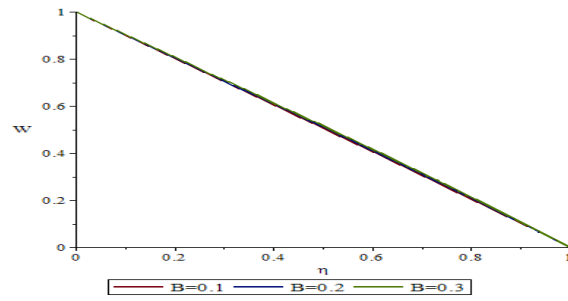


Figure 8: Variation of B on W

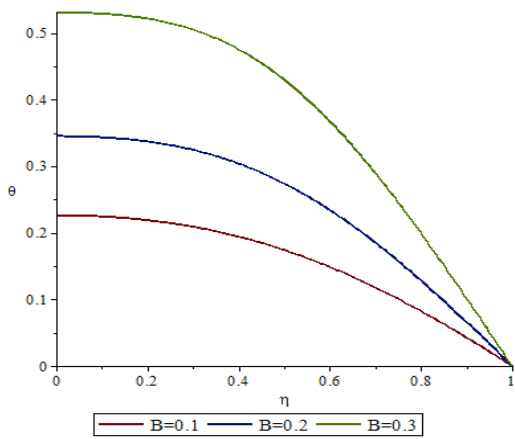


Figure 9: Variation of B on θ

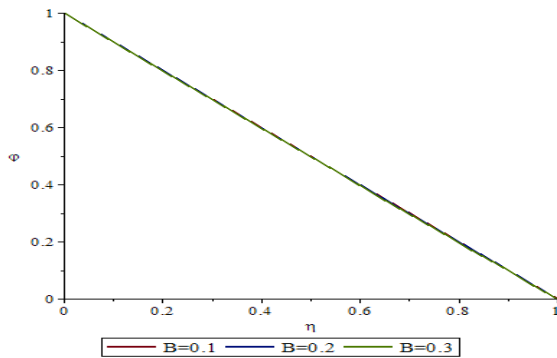


Figure 10: Variation of B on W

Figures 1 to 5 depict the effects of rotational parameter on radial, tangential, axial velocity, temperature and concentration profiles respectively. As the rotational parameter increases, the radial and axial velocity get boosted while the tangential velocity decreases. The fluid temperature dropped and a slight increase in the concentration is observed.

Figures 6 to 10 is the variation of FHD interactive parameter on the velocity, temperature and

concentration profiles respectively. The FHD parameter is observed to be an increasing agent on the fluid radial, axial velocity and a reducing agent on the tangential velocity. The fluid temperature is seen to raise high on the wall surface with increase in FHD parameter and drop to zero at free stream while the fluid concentration also increases.

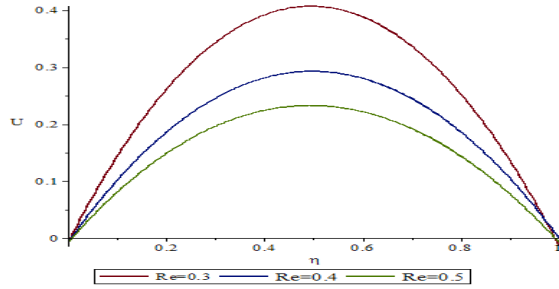


Figure 11: Variation of Re on U

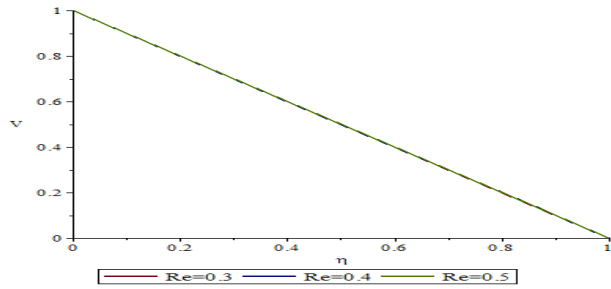


Figure 12: Variation of Re on V

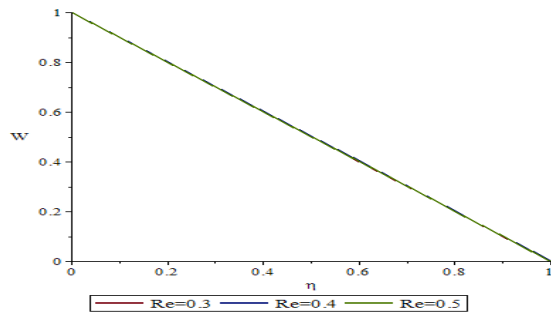


Figure 13: Variation of Re on W

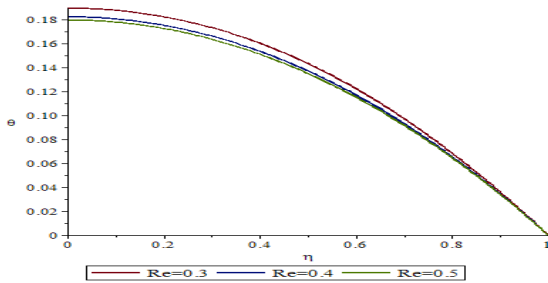


Figure 14: Variation of Re on θ

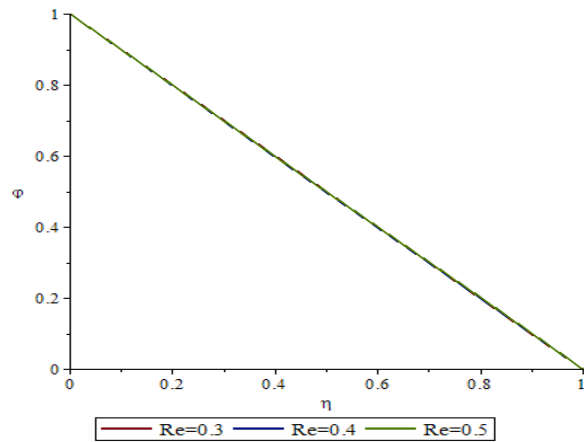


Figure 15: Variation of Re on φ

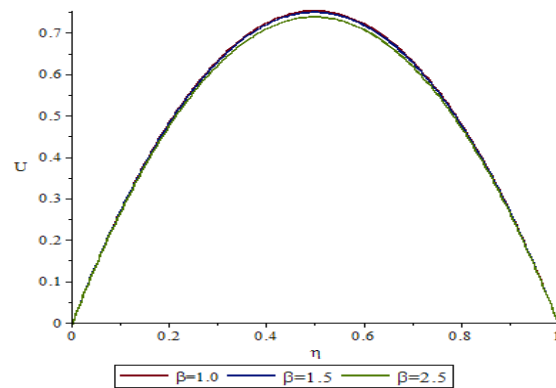


Figure 16: Variation of β on U

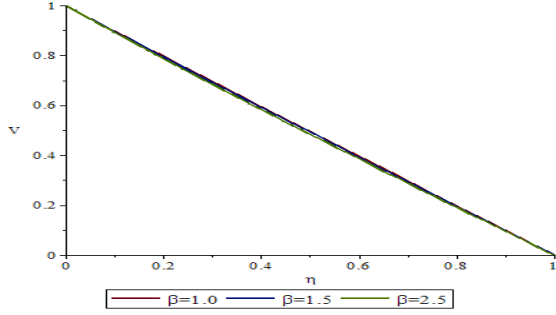


Figure 17: Variation of β on V

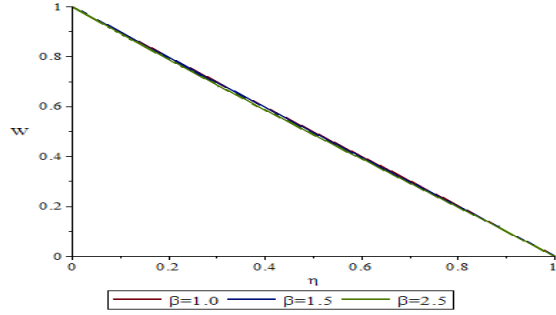


Figure 18: Variation of β on W

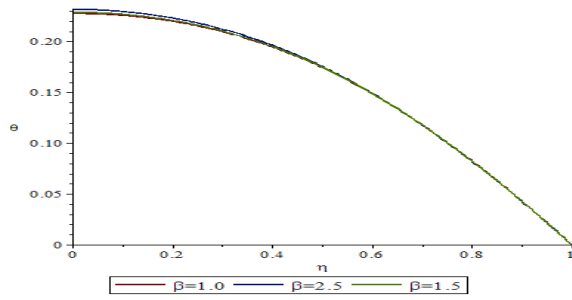


Figure 19: Variation of β on θ

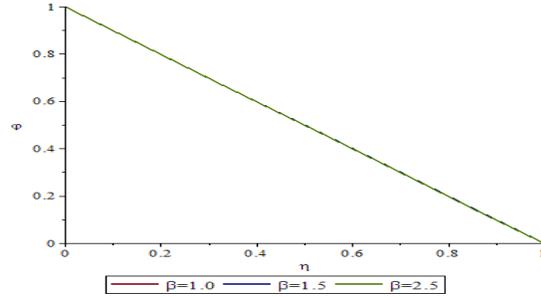


Figure 20: Variation of β on φ

Table 1: Comparison of $U_{\eta\eta}(0)$ with β when $B = R = Re = 1$

β	[14]	Present results
0.5	-0.605825	-0.630321599
1.5	-0.59867	-0.597171257
2	-0.592452	-0.585886645
3	-0.577199	-0.56640511

Figures 16 to 20 indicate the influence of Darcy number on the fluid velocity Temperature and concentration profiles respectively. As the Darcy number thickens, radial velocity also dropped while the tangential and axial velocity thickens. This causes

loss in momentum in the radial velocity and gain in momentum in the case of tangential and axial velocity which is as a result of Kevin force from the magnetic field. The fluid temperature and concentration are enhanced.

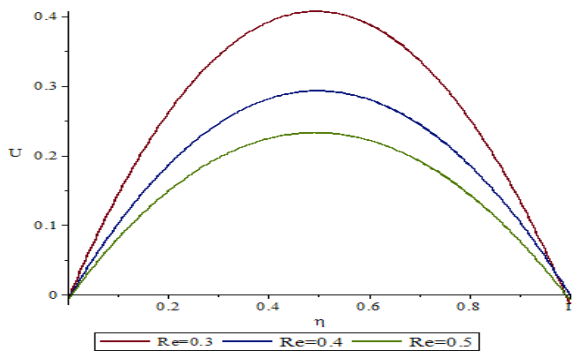


Figure 21: Variation of Re on U

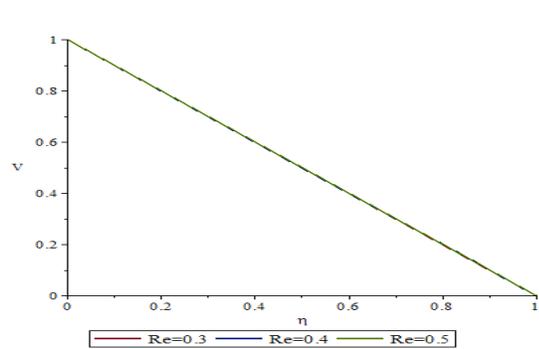


Figure 22: Variation of Re on V

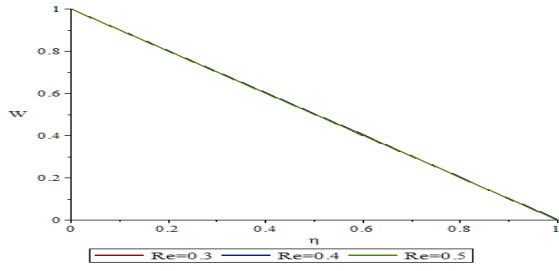


Figure 23: Variation of Re on W

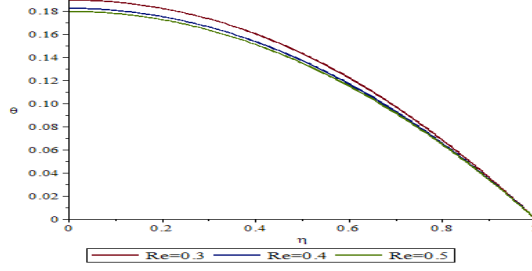


Figure 24: Variation of Re on θ

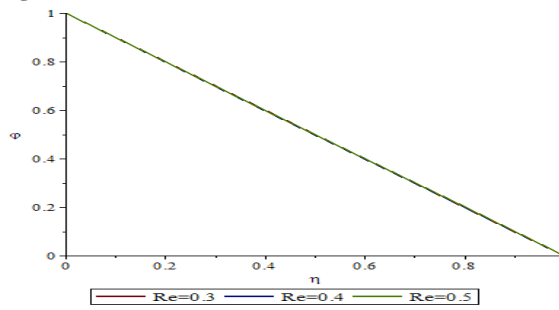


Figure 25: Variation of Re on φ

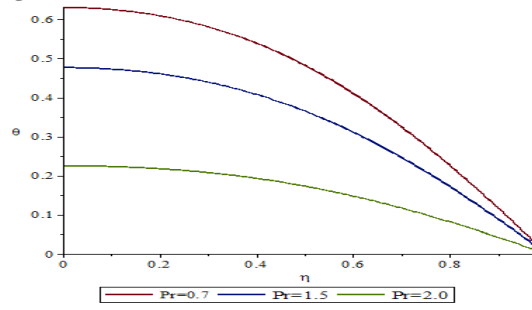


Figure 26: Variation of Pr on θ

Figures 21 to 25 displayed the variation of Reynolds number on the radial, tangential, axial velocity, temperature and concentration profiles respectively. Increase in Reynolds number decreases the radial

velocity and increases the tangential and axial velocity of the fluid. It also causes a drop in the temperature while concentration is enhanced.

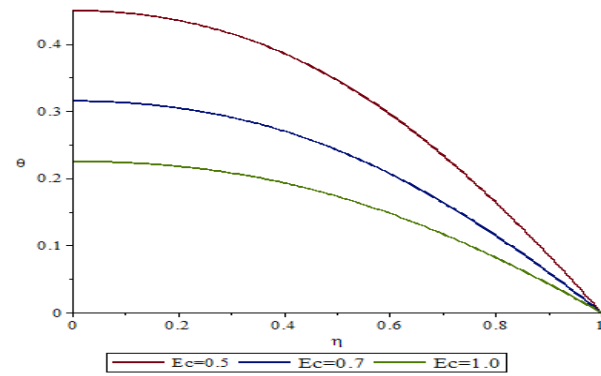


Figure 27: Variation of Ec on θ

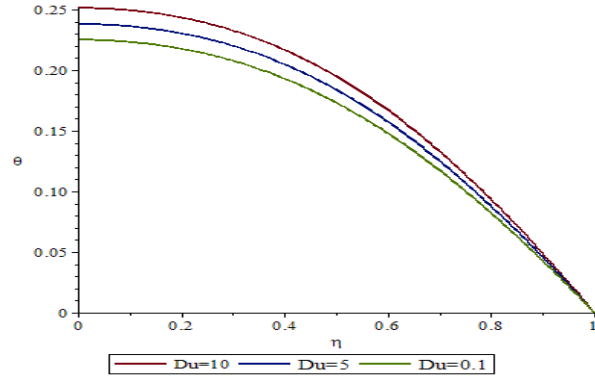


Figure 28: Variation of Du on θ

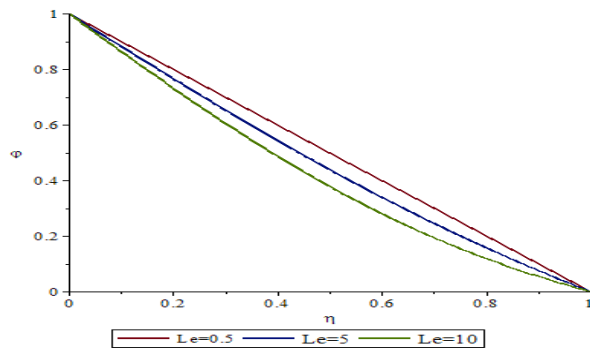


Figure 29: Variation of Le on φ

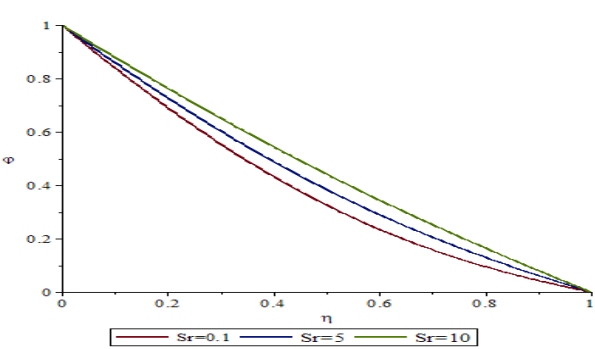


Figure 30: Variation of Sr on φ

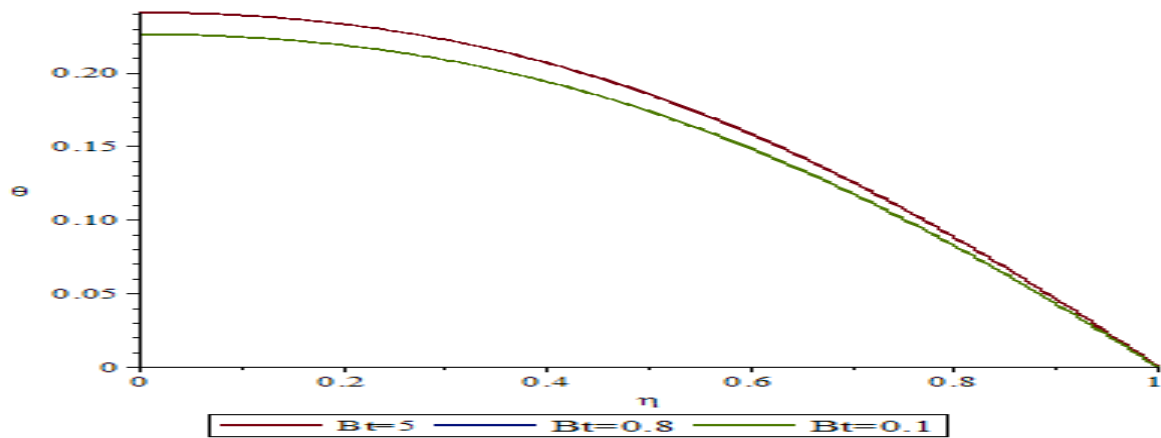


Figure 31: Variation of Bt on θ

Figures 26 to 28 present the variation of Prandtl number, Eckert number and Dufour number on the fluid temperature respectively. As Prandtl number increases, the fluid temperature is observed to lose momentum which result to reduction in temperature of the fluid. Eckert number is found to be an increasing agent of the fluid temperature which is due to viscosity. When temperature rises, the fluid viscosity also rise. Dufour is found to be an increasing agent of the fluid temperature.

Figure 29 to 30 display the graph of Lewis number and Soret number on the fluid concentration respectively. Increase Lewis number causes the fluid concentration to decrease while the Soret number is found to enhance the fluid concentration. Figure 31 shows the effect of Biot number on temperature profile and it is found to increase the fluid temperature as it gets boosted.

CONCLUSION

Sharma *et al.* (2021) is considered in this work by the introduction of concentration and Dufour, Soret and Convective boundary condition. The formulated problems were solved using decomposition method and the results obtained were compared with literature. The work is hereby concluded with the following observations:

1. The Dufour number increases the temperature profile while Soret number increases the fluid concentration significantly.
2. Biot number is found to enhance the fluid temperature.
3. The graphs presented in this work all satisfy both the initials and the boundary conditions which depict that the problem is well poss.
4. All other parameters were kept constant while a parameter is varied.

5. The radial, tangential, axial velocity, temperature and concentration all decayed to zero at free stream.

REFERENCES

- Al-Hadhrami, A.K., Elliott, L. and Ingham, D.B. (2003). A new model for viscous dissipation in porous media across a range of permeability values. *Transportation in a Porous Media*, 53:117-22.
- Aiyesimi, Y. M. Yusuf, A. and Jiya, M. (2013). A Hydromagnetic Boundary Layer Micropolar Fluid over a Stretching Surface in a Non-Darcian Medium with Permeability. Horizon Research Publishing, *Universal Journal of Applied Mathematics (UJAM)*, 1(2): 136-141. DOI: 10.13189/ujam.2013.010216.
- Bolarin, G., Yusuf, A., Adekunle, S. T., Aiyesimi, Y. M. and Jiya, M. (2019). Analysis of a Boundary Layer Flow of Nanofluid Over an Inclined Plane Via ADM. *Sigma Journal of Engineering and Natural Sciences*, 37 (2): 475-488.
- Chen, C. H. (2010). Combined effects of joule heating and viscous dissipation on magneto hydrodynamic flow past a permeable, stretching surface with free convection and radiative heat transfer. *ASME Journal of Heat Transfer*, 132(6):064503.
- Devi, S.P.A. and Ganga, B. (2009). Effects of viscous and joules dissipation on MHD flow, heat and mass transfer past a stretching porous surface embedded in a porous medium. *Nonlinear Analysis*, 14(3):303-14.

- Herrero, J., Humphrey, J.A.C. and Giralt, F. (1994). Comparative analysis of coupled flow and heat transfer between corotating discs in rotating and fixed cylindrical enclosures. *American Society of Mechanical Engineering Heat Transfer Division*, 300: 111–21.
- Khan, M.I. and Alzahrani, F. (2021). Nonlinear dissipative slip flow of jeffrey nanomaterial towards a curved surface with entropy generation and activation energy. *Mathematical Computation and Simulation*, 185: 47–61.
- Maleque, K.H.A. (2010). Effects of combined temperature- and depth-dependent viscosity and hall current on an unsteady MHD laminar convective flow due to a rotating disk. *Chemical Engineering Communications*, 197(4):506–21.
- Sharma, R. (2012). Effect of viscous dissipation and heat source on unsteady boundary layer flow and heat transfer past a stretching surface embedded in a porous medium using element free Galerkin method. *Applied Mathematical Computation*. 219(3):976–87.
- Sharma, K , Vijaya , N., Makinde, O. D., Bhardwaj, S.B., Singhd, R. M. and Mabood, F. (2021). Boundary layer flow with forced convective heat transfer and viscous dissipation past a porous rotating disk. *Chaos, Solitons and Fractals*, 148: 111055.
- Suleiman, A. and Yusuf, A. (2020). Analytical study of heat transfer on flow of a nanofluid in a porous medium with heat generation. *Journal of Science, Technology, Mathematics and Education (JOSMED)*, 16(3): 49-57.
- Turkyilmazoglu, M. (2014). Nanofluid flow and heat transfer due to a rotating disk. *Computational Fluid*, 94:139–46.
- Yusuf, A., Gupa, M. I., Sayeed, N. H. and Bolarin, G. (2021a). Thermo-Diffusion effects of a stagnation point flow in a nanofluid with convection using Adomian decomposition Method. *Covenant Journal of Physical & Life Sciences (CJPL)*, 9(20): 2354-3574.
- Yusuf, A., Sayeed, N. H., Salisu, A., Onwuzurike, B. and Bolarin, G. (2021b). Analysis of Thermo-diffusion and its effects in an inclined hydromagnetic boundary layer flow due to radial stretching with convective boundary conditions, *Lapai Journal of Applied and Natural Sciences (LAJANS)*, 6(1):131-136.